

Magnetocaloric effect in exchange-coupled strong/weak/strong ferromagnet stacks

Cite as: J. Appl. Phys. **127**, 183904 (2020); <https://doi.org/10.1063/5.0003223>

Submitted: 31 January 2020 . Accepted: 20 April 2020 . Published Online: 12 May 2020

M. A. Kuznetsov, I. Y. Pashenkin, N. I. Polushkin , M. V. Sapozhnikov , and A. A. Fraerman

COLLECTIONS

Paper published as part of the special topic on [Multicalorics](#)

Note: This paper is part of the Special Topic on Multicalorics.



[View Online](#)



[Export Citation](#)



[CrossMark](#)

ARTICLES YOU MAY BE INTERESTED IN

[Electron dynamics in low pressure capacitively coupled radio frequency discharges](#)
Journal of Applied Physics **127**, 181101 (2020); <https://doi.org/10.1063/5.0003114>

[Spin-wave filters based on thin \$\text{Y}_3\text{Fe}_5\text{O}_{12}\$ films on \$\text{Gd}_3\text{Ga}_5\text{O}_{12}\$ and Si substrates for microwave applications](#)
Journal of Applied Physics **127**, 183903 (2020); <https://doi.org/10.1063/5.0007338>

[Three terminal nano-oscillator based on domain wall pinning by track defect and anisotropy control](#)
Journal of Applied Physics **127**, 183905 (2020); <https://doi.org/10.1063/1.5144691>

Lock-in Amplifiers
up to 600 MHz



Magnetocaloric effect in exchange-coupled strong/weak/strong ferromagnet stacks

Cite as: J. Appl. Phys. 127, 183904 (2020); doi: 10.1063/5.0003223

Submitted: 31 January 2020 · Accepted: 20 April 2020 ·

Published Online: 12 May 2020



View Online



Export Citation



CrossMark

M. A. Kuznetsov,^{1,2,a)} I. Y. Pashenkin,¹ N. I. Polushkin,¹ M. V. Sapozhnikov,¹ and A. A. Fraerman^{1,a)}

AFFILIATIONS

¹Institute for Physics of Microstructures, Russian Academy of Sciences, Akademicheskaya St. 7, Nizhny Novgorod 607680, Russian Federation

²Lobachevsky State University of Nizhny Novgorod, Faculty of Physics, 23 Gagarin Av., Nizhny Novgorod 603950, Russian Federation

Note: This paper is part of the Special Topic on Multicalorics.

a) Authors to whom correspondence should be addressed: mikhail5340@gmail.com and andr@ipmras.ru

ABSTRACT

We study the magnetocaloric effect in layered systems composed of a ferromagnet with a relatively low Curie temperature (T_C), which is sandwiched by stronger ferromagnets and exchange coupled to them across the interfaces. Switching of magnetization in the softer ferromagnetic surrounding in an applied magnetic field (H) of the strength in several tens of oersteds provides the isothermal magnetic entropy change (Δs) in the system because of magnetization redistribution in the spacer. Our simulations of these effects we present here reveal the maximal value of Δs , obtained at a realistic interfacial exchange constant, which is in quantitative agreement with this quantity observed experimentally in different heterosystems based on the $\text{Ni}_x\text{Cu}_{100-x}$ ($x \sim 70$ at. %) spacer.

Published under license by AIP Publishing. <https://doi.org/10.1063/5.0003223>

I. INTRODUCTION

The magnetocaloric effect (MCE) is believed to be sufficient by applying a magnetic field (H) up to several tens of kilo-oersteds near the point of phase magnetic transition in the refrigerant, e.g., near Curie temperature (T_C).^{1–6} However, such strong magnetic fields can be produced by bulky magnets that cannot be convenient for usage in magnetic refrigeration. In our work, we study whether it is possible to achieve the robust MCE by applying very weak magnetic fields, e.g., several tens of oersteds. The system of our interest is a heterostructure composed of a thin (~ 10 nm) spacer (refrigerant) between ferromagnetic layers that have higher Curie temperatures.^{7–10} A magnetic field of $H \sim 10^2$ Oe applied to such a system induces switching of magnetization in the magnetically softer surrounding. Due to exchange coupling across the interfaces with the surroundings, this reconfiguration mediates the redistribution of magnetization in the spacer and thus the isothermal magnetic entropy change (Δs) in the system. Schematically, spacer magnetization $m(z)$ under the parallel ($\uparrow\uparrow$) and antiparallel ($\uparrow\downarrow$) orientations of magnetizations in the surroundings is shown in Fig. 1.

As previously predicted for the magnetocaloric properties of these systems,¹¹ the magnetocaloric potential is

$$\Delta s = m_s^2/C, \quad (1)$$

where m_s is the saturation magnetization of the spacer and C is the Curie constant. Equation (1) adequately describes the behavior of real systems under the condition that the spacer can be magnetized up to m_s at the interfaces. For example, in a heterostructure system based on the $\text{Ni}_x\text{Cu}_{100-x}$ ($x \sim 70$ at. %) spacer,¹² the magnetocaloric potential can achieve $\Delta s = 10^5 \text{ erg/cm}^3 \text{ K}$ at $4\pi m_s = 2.5 \text{ kG}$ and $C = 0.4 \text{ K}$ taken for $\text{Ni}_{72}\text{Cu}_{28}$.¹³ So the adiabatic temperature change is expected to be $\Delta T = T_C \Delta s / c_v = 0.6 \text{ K}$, where $T_C = 300 \text{ K}$ and $c_v = 5.0 \times 10^7 \text{ erg/cm}^3/\text{K}$ ¹⁴ is the heat capacity of the spacer near T_C .

Here, we simulate the magnetization distribution across the spacer under $\uparrow\uparrow$ and $\uparrow\downarrow$ orientations of magnetizations in the surroundings. These simulations allow us to correctly evaluate the magnetocaloric potential of the system under study. The theoretical results mentioned above are presented in Sec. II. In Sec. III, we

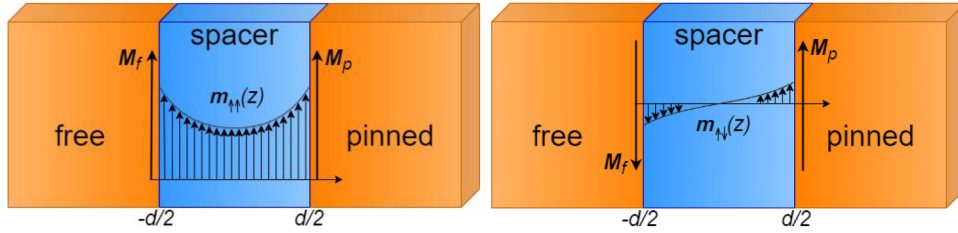


FIG. 1. Spacer magnetization $m(z)$ under parallel ($\uparrow\uparrow$) (left) and antiparallel ($\uparrow\downarrow$) (right) orientations of magnetizations in the surroundings. A change in $m(z)$ due to switching of the soft (free) ferromagnetic surrounding leads to the isothermal magnetic entropy change (Δs) that should provide the MCE at temperatures close to T_C .

collect magnetization curves of different $\text{Ni}_x\text{Cu}_{100-x}$ -based heterostructure systems (with one of the surroundings both unpinned and pinned with an antiferromagnetic layer^{7–10}) and give our explanations about how the collected data are helpful to retrieve the magnetocaloric potential of the studied samples. Finally, in Sec. IV, we compare the obtained experimental data with the results of our simulations.

II. MCE MODELING

The calculation was performed in terms of the phenomenological Landau theory for second-type phase transitions. The free energy per area unit of a paramagnetic ($T > T_C$) spacer, whose magnetization is $m(z)$ and is sandwiched by ferromagnetic surroundings, can be written as¹¹

$$F = \int_{-d/2}^{d/2} \{(\alpha\tau/2)m^2 + (\beta/4m_s^2)m^4 + (l_0^2/2)(dm/dz)^2\} dz + \frac{1}{2} l_j(m - \sigma m_s)^2|_{z=-d/2} + \frac{1}{2} l_j(m - m_s)^2|_{z=d/2}, \quad (2)$$

with the boundary conditions as follows

$$\begin{aligned} dm/dz &= (l_j/l_0^2)(m - \sigma m_s)|_{z=-d/2}, \\ dm/dz &= -(l_j/l_0^2)(m - m_s)|_{z=d/2}, \end{aligned} \quad (3)$$

where $l_0 = (2A)^{1/2}/m_s$ is the exchange constant inside the spacer in units of length (cm), A is the exchange stiffness in units of energy/length (erg/cm), $l_j = E_\sigma/m_s M_f$ is the exchange constant in units of length (cm) at the interface between the spacer and soft surrounding, E_σ is the interfacial exchange energy per area unit, M_f is the saturation magnetization in the soft surrounding, $\tau = (T - T_C)/T_C$, and $\sigma = \pm 1$ for the parallel (upper sign) and antiparallel (lower sign) configurations of the magnetizations. The equation that corresponds to the minimum for the functional in Eq. (2) reads

$$d^2m/dz^2 - l^{-2}m - \beta l_0^{-2}m_s^{-2}m^3 = 0, \quad (4)$$

where $l = l_0/(\alpha\tau)^{1/2}$. Solutions of Eq. (4) can be sought as $m_{\uparrow\uparrow} = a_{\uparrow\uparrow}m_s \operatorname{dn}(c_{\uparrow\uparrow}z/l_0, k_{\uparrow\uparrow})$ and $m_{\uparrow\downarrow} = (a_{\uparrow\downarrow}^{1/2}m_s/c_{\uparrow\downarrow}) \operatorname{sn}(c_{\uparrow\downarrow}z/l_0, k_{\uparrow\downarrow})$, where $\operatorname{dn}(u, k)$ and $\operatorname{sn}(u, k)$ are Jakobi elliptic functions having the

well-known properties¹⁵ and $k_{\uparrow\uparrow(\uparrow\downarrow)}$ are the elliptic modules. The dimensionless constants $a_{\uparrow\uparrow(\uparrow\downarrow)}$ and $c_{\uparrow\uparrow(\uparrow\downarrow)}$, which are in direct relationship each with other, can be found from the boundary conditions (3). Substituting $m_{\uparrow\uparrow}$ and $m_{\uparrow\downarrow}$ into Eq. (4), we obtain that

$$\begin{aligned} m_{\uparrow\uparrow} &= a_{\uparrow\uparrow}m_s \operatorname{dn}\left(ia_{\uparrow\uparrow}\sqrt{\beta/2}z/l_0, \sqrt{2(1 + \frac{\alpha\tau}{\beta a_{\uparrow\uparrow}^2})}\right), \\ m_{\uparrow\downarrow} &= -i\left(2\frac{a_{\uparrow\downarrow}}{\beta}\right)^{1/4} \lambda m_s \operatorname{sn}\left(i\left(\frac{\beta a_{\uparrow\downarrow}}{2}\right)^{1/4} \frac{z}{\lambda l_0}, \sqrt{-1 + 2\tau_0\lambda^2}\right), \end{aligned} \quad (5)$$

where $\lambda = (\tau_0 + (\tau_0^2 - 1)^{1/2})^{1/2}$, $\tau_0 = \alpha\tau/(2\beta a_{\uparrow\uparrow})^{1/2}$, and i is the imaginary unit.

Figure 2(a) shows the magnetization distributions $m_{\uparrow\uparrow}(z)$ and $m_{\uparrow\downarrow}(z)$, which were found from Eq. (5) for the spacers of different thicknesses, from $d = 15$ nm to $d = 3$ nm. For these calculations, the following material parameters were taken: $4\pi m_s = 2.5$ kG (for $\text{Ni}_{72}\text{Cu}_{28}$),¹³ $l_0 = 25$ nm, $A = 1.0 \times 10^{-7}$ erg/cm,¹⁶ $E_\sigma = 0.775$ erg/cm² and $l_j = 30$ nm,^{17,18} and $4\pi M_f = 16.5$ kG (for CoFeB),¹⁹ while the constants α and β in the functional of Eq. (2) are retrievable by fitting the equation $\alpha\tau m + (\beta/m_s^2)m^3 = H$ ²⁰ to the experimental data, which were reported in Ref. 21 for a thin $\text{Ni}_{67}\text{Cu}_{33}$ film.

The magnetocaloric potential $\Delta s = s_{\uparrow\downarrow} - s_{\uparrow\uparrow}$ can be derived by substitution of $m_{\uparrow\uparrow}(z)$ and $m_{\uparrow\downarrow}(z)$ [Eq. (5)] into the functional of Eq. (2)—with taking into account that $s_{\uparrow\uparrow(\uparrow\downarrow)} = -(\partial F_{\uparrow\uparrow(\uparrow\downarrow)}/\partial T)/d$. As a result, we find that

$$\begin{aligned} s_{\uparrow\uparrow} &= -\frac{\alpha l_0 a_{\uparrow\uparrow}^2 m_s^2}{T_C c_{\uparrow\uparrow} d} E\left(\operatorname{am}\left(\frac{c_{\uparrow\uparrow} d}{2l_0}, k_{\uparrow\uparrow}\right), k_{\uparrow\uparrow}\right), \\ s_{\uparrow\downarrow} &= -\frac{\alpha a_{\uparrow\downarrow} m_s^2}{2T_C c_{\uparrow\downarrow}^2 k_{\uparrow\downarrow}^2} \left(1 - \frac{2l_0}{c_{\uparrow\downarrow} d} E\left(\operatorname{am}\left(\frac{c_{\uparrow\downarrow} d}{2l_0}, k_{\uparrow\downarrow}\right), k_{\uparrow\downarrow}\right)\right), \end{aligned} \quad (6)$$

where $E(u, k)$ is the second-type elliptic integral and $\operatorname{am}(u, k)$ is the first-type elliptic integral amplitude.

In Fig. 2(b) we show Δs as a function of T at different thicknesses d of the spacer. We see that Δs monotonously increases with decreasing d . As seen from Fig. 2(a), $m_{\uparrow\uparrow}$ is not large ($< 0.3m_s$) even in a thin spacer ($d = 3$ nm) exposed to the exchange field of $E_\sigma/$

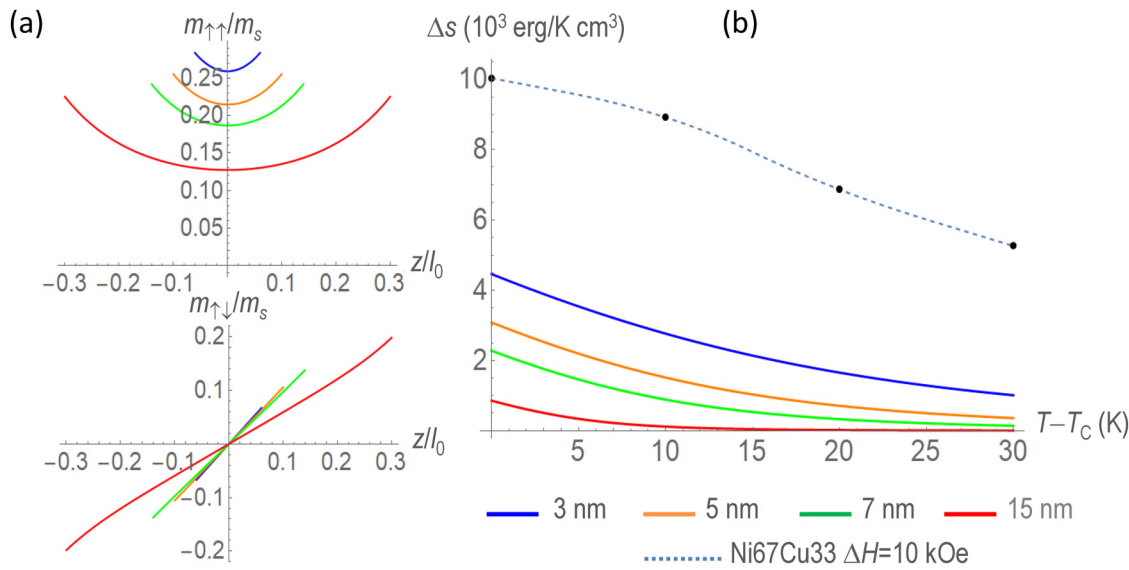


FIG. 2. (a) Simulated distributions $m_{\uparrow\uparrow}^{\dagger\dagger}(z)$ and $m_{\uparrow\downarrow}^{\dagger\dagger}(z)$ at $T = T_c$ in spacers with different thicknesses $d = 3$ nm, 5 nm, 7 nm, and 15 nm. The magnetization profiles were calculated at $E_\sigma = 0.775 \text{ erg/cm}^2$ and $l_0 = 30 \text{ nm}$,^{17,18} which is the critical parameter. (b) Corresponding values of $\Delta s = s_{\uparrow\downarrow} - s_{\uparrow\uparrow}$ vs $T - T_c$. For comparison, the magnetocaloric potential Δs is shown for a thin Ni₆₇Cu₃₃ film exposed to a magnetic field H varied from 0.0 kOe to 10 kOe.²¹

$M_f d = 200$ kOe. Nevertheless, the maximal Δs achievable at $T = T_c$ is only twice lower (in the $d = 3$ nm spacer) than the magnetocaloric potential of a Ni₆₇Cu₃₃ film exposed to a magnetic field of 10 kOe.²¹ As one expects to obtain such a value of Δs in the heterostructure system exposed to a magnetic field of $H \sim 0.1$ kOe only¹² (see also the experimental part here, Sec. III, which supports this expectation), the magnetocaloric efficiency in a Ni_xCu_{100-x}-based ($x \sim 70$ at. %) system can be enhanced up to ~ 50 times by comparison to that in a separate Ni_xCu_{100-x} film.

III. EXPERIMENT

The experiments were performed with two types of heterostructure systems in which the Ni_xCu_{100-x} spacer was used as the key component (refrigerant). One of the systems under study (S1) was quartz substrate/(10 nm)Py/(d nm)Ni₆₇Cu₃₃/(3 nm)Co₉₀Fe₁₀/(25 nm)Ir₂₀Mn₈₀/TiO (Py = Ni₈₀Fe₂₀) stacks,¹² where the Py layer was magnetically soft, while another ferromagnetic surrounding, Co₉₀Fe₁₀ (CoFe), was pinned with the antiferromagnetic layer of Ir₂₀Mn₈₀.⁷⁻¹⁰ Another system (S2) was Si substrate/(20 nm)

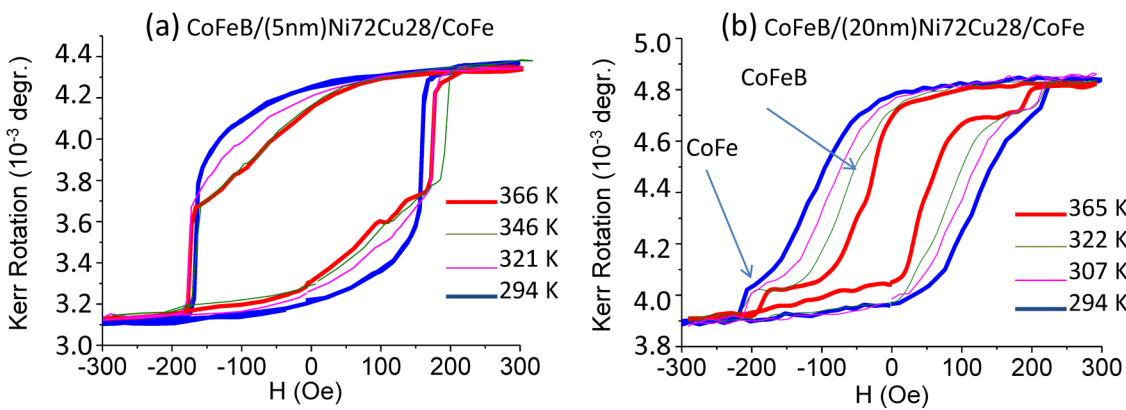


FIG. 3. MOKE hysteresis loops for a (15 nm)CoFeB/Ni₇₂Cu₂₈/(20 nm)CoFe heterostructure system (S2) with spacer thicknesses of $d = 5$ nm (a) and $d = 20$ nm (b). Magnetizations in the soft CoFeB and hard CoFe surroundings are switchable by applying different magnetic fields H . The stronger the dependence of H_{sw} on T , the higher the magnetocaloric efficiency.¹²

$\text{Co}_{90}\text{Fe}_{10}/(d \text{ nm})\text{Ni}_{72}\text{Cu}_{28}/(15 \text{ nm})\text{Co}_{40}\text{Fe}_{40}\text{B}_{20}/\text{TiO}$ stacks—with the hard CoFe and soft $\text{Co}_{40}\text{Fe}_{40}\text{B}_{20}$ (CoFeB) ferromagnetic surroundings. The details for sample preparation were given in Ref. 12.

The magnetic and magnetocaloric properties of prepared samples were studied with a Lake Shore 7400 Series vibrating sample magnetometer¹² as well as with a home-built setup based on the longitudinal magneto-optical Kerr effect (MOKE). Figure 3 shows magnetization curves taken by MOKE for two samples of the system S2 with spacer thicknesses of $d = 5 \text{ nm}$ (a) and $d = 20 \text{ nm}$ (b). These measurements were performed in a temperature range above room temperature. In particular, we find that the ferromagnetic surroundings we use in system S2 have strongly different switching fields. Indeed, magnetization of the soft CoFeB surrounding toggles in a magnetic field H_{sw} varying in a range from a few oersteds to a few tens of oersteds, which depends on T , while the start for the switching of the pinned CoFe layer delays up to $H \sim 180 \text{ Oe}$. This behavior of system S2 is similar to that of system S1. The latter system was also studied in Ref. 12.

In the context of our study, it is important to note that the start of magnetization switching in the soft surrounding depends on T : H_{sw} increases with lowering T . *The derivative of H_{sw} on T straightforwardly relates to the magnetocaloric efficiency of the system.*¹² This can be understood in a frame of the phenomenological model for interlayer exchange between two ferromagnetic layers that have different switching fields in an applied magnetic field H . The effective free energy of this system can be written as $F_{eff} = -J\mathbf{M}_f\mathbf{M}_p - \mathbf{M}_f\mathbf{H}$, where \mathbf{M}_f and \mathbf{M}_p are magnetization vectors of the soft (free) and hard (pinned) ferromagnets, respectively, which aligned in the same (opposite) direction(s) at $H < H_{sw}$ ($H > H_{sw}$). In this form, the first term reflects interlayer exchange J , which depends on T . One anticipates that the $J(T)$ dependence is especially strong at $T \rightarrow T_C$. If, roughly speaking, magnetization of the free layer is a step function of H , i.e., $M = M_f\theta(H - JM_p)$, then the magnetic entropy changes abruptly at $H = H_{sw} = JM_p$ and this change is $\Delta s = 2M_pM_f\partial J/\partial T$.^{12,22}

Upon that basis and taking into account that $M_f \gg m$, so that the free surrounding mostly contributes to the switching, we obtain that the magnetocaloric potential of the spacer is as follows:^{12,22}

$$\Delta s = \frac{h_f}{d} \int_{H_{sw}-\epsilon_1}^{H_{sw}+\epsilon_2} \left(\frac{dM}{dT} \right) dH, \quad (7)$$

where h_f is the thickness of the free surrounding and $\epsilon_{1,2}$ the edges of integration. Thus, the values of Δs were retrieved by processing the magnetization curves with the help of Eq. (7). In order to find Δs from the MOKE hysteresis loops shown in Fig. 3, we assumed that $4\pi M_f = 16.5 \text{ kG}$.¹⁹

IV. COMPARISON BETWEEN THEORY AND EXPERIMENT

Figure 4 shows obtained experimental values of Δs vs T for the samples of both types, S1 and S2. We find that Δs is a non-monotonous function of T and has the maximum at T_C ,¹² which

shifts toward higher T with increasing Ni content in the spacer. We see that in system S2, for example, the maximal magnetocaloric potential is $\Delta s \approx 3.3 \times 10^3 \text{ erg/cm}^3/\text{K}$ at $T = T_C$. In the same plot, we show the values of Δs at the theoretical limit given by Eq. (1) as well as the magnetic potential of a separate film from the spacer material ($\text{Ni}_{67}\text{Cu}_{33}$) in the field region between $H = 0 \text{ Oe}$ and $H = 30 \text{ Oe}$. The values of Δs for a separate $\text{Ni}_{67}\text{Cu}_{33}$ film were retrieved by extrapolation of the data obtained in Ref. 21 into the region of low H . For extrapolation, the edge value for the field range of interest was taken equal to the switching field of the soft surrounding in system S1, $H_{sw} = 30 \text{ Oe}$.¹² Although the magnetocaloric potential of the heterostructure system is much higher than that of a separate $\text{Ni}_{67}\text{Cu}_{33}$ film exposed to H up to 30 Oe, it is still significantly (≈ 30 times) lower than the theoretical limit for Δs , which is given by Eq. (1).

However, it here is of central importance to compare Δs obtained in real systems with the theoretical values of this quantity [Fig. 2(b)] retrievable at a realistic value of the interfacial exchange constant J_f .^{17,18} We find that the maximal value of Δs at $T = T_C$ obtained experimentally for system S2 agrees well with the theoretical one calculated for the $d = 5 \text{ nm}$ spacer. We see, however, that the theoretical $\Delta s(T)$ dependence is significantly sharper than the experimental one. For example, at $T - T_C = 20 \text{ K}$, the theoretical value of Δs is nearly three times smaller than the experimental one. It is likely that this disagreement results from the limitation of the Landau theory for the second-type phase transition, which is used in our simulations, at temperatures far enough from T_C .

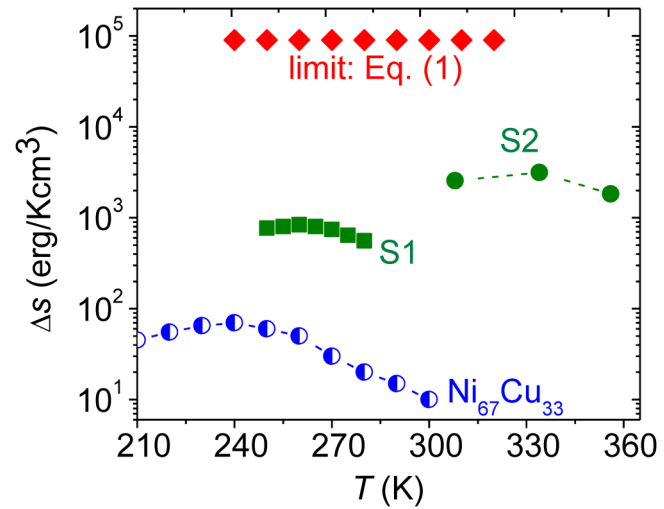


FIG. 4. Experimental $\Delta s(T)$ dependences for the heterostructure systems S1 and S2. The obtained values of Δs have been compared to this quantity simulated at a realistic interfacial exchange constant $J_f = 30 \text{ nm}$ ^{17,18} for $d = 5 \text{ nm}$ [Fig. 2(b)]. The values of Δs at the theoretical limit given by Eq. (1) and for a separate $\text{Ni}_{67}\text{Cu}_{33}$ film in the field range of 0–30 Oe are also shown. The $\Delta s(T)$ dependence for a separate film from the spacer material was found by extrapolation of the data obtained from Ref. 21.

V. SUMMARY

We propose a system in which the robust MCE is anticipated by applying very weak magnetic fields $H \sim 10^2$ Oe. This system consists of a paramagnetic (or weak ferromagnetic) layer (refrigerant), which is sandwiched by layers of strong ferromagnets. According to a phenomenological model for interlayer exchange, switching of the soft (free) surrounding at $H = H_{sw}$ provides the isothermal magnetic entropy change proportional to the temperature derivative of the interlayer exchange constant (dJ/dT). In our experiments, we use $\text{Ni}_x\text{Cu}_{100-x}$ ($x \sim 70$ at. %) alloys as paramagnetic spacers between magnetically soft (Py or CoFeB) and hard (CoFe) surroundings. By measuring their magnetization curves at different temperatures, we take interest in how strongly switching of magnetization in the soft surrounding is sensitive to variation of temperature near the Curie point of the spacer (T_C). This sensitivity reflects the magnetocaloric efficiency of the system. We find that, although the experimental values of ΔS in the heterostructure systems are significantly higher than that of a separate $\text{Ni}_x\text{Cu}_{1-x}$ film, the theoretical limit (when the spacer is magnetized up to saturation at the interfaces) is still essentially higher (by a factor of ~ 30) than that observed experimentally. In order to explain the smallness of experimental ΔS , we have modeled the distributions of spacer magnetization, $m_{\uparrow\uparrow}(z)$ and $m_{\uparrow\downarrow}(z)$, for the parallel ($\uparrow\uparrow$) and antiparallel ($\uparrow\downarrow$) orientations of magnetizations in the surroundings at a realistic value of the interfacial exchange constant. In these simulations, we have found that magnetization of a $\text{Ni}_x\text{Cu}_{100-x}$ spacer is far from its saturation even at the interfaces. The maximal value of ΔS that corresponds to the calculated $m_{\uparrow\uparrow}(z)$ and $m_{\uparrow\downarrow}(z)$ dependences is found to be compatible with this quantity observed experimentally.

ACKNOWLEDGEMENTS

This work was supported by the Russian Foundation for Basic Research (Grant No. 20-02-00356) and by the Ministry of Education and Science of Russian Federation (Grant No. 0035-2019-0022-C-01).

REFERENCES

- ¹A. M. Tishin and Y. I. Spichkin, *The Magnetocaloric Effect and Its Application* (IOP Publishing Ltd., 2003).
- ²A. Gschneidner, Jr., V. K. Pecharsky, and A. O. Tsokol, “Recent developments in magnetocaloric materials,” *Rep. Prog. Phys.* **68**, 1479–1539 (2005).
- ³V. Basso, C. P. Sasso, and M. Küperling, “Entropy change at magnetic phase transitions of the first order and second order,” *Int. J. Refrig.* **37**, 257–265 (2014).
- ⁴M. Balli, S. Jandl, P. Fournier, and A. Kedous-Lebouc, “Advanced materials for magnetic cooling: Fundamentals and practical aspects,” *Appl. Phys. Rev.* **4**, 021305 (2017).
- ⁵J. Lyubina, “Magnetocaloric materials for energy efficient cooling,” *J. Phys. D Appl. Phys.* **50**, 053002 (2017).
- ⁶V. Franco, J. S. Blázquez, J. J. Ipus, J. Y. Law, L. M. Moreno-Ramírez, and A. Conde, “Magnetocaloric effect: From materials research to refrigeration devices,” *Prog. Mater. Sci.* **93**, 112–232 (2018).
- ⁷A. F. Kravets, A. N. Timoshevskii, B. Z. Yanchitsky *et al.*, “Temperature-controlled interlayer exchange coupling in strong/weak ferromagnetic multilayers: A thermomagnetic Curie switch,” *Phys. Rev. B* **86**, 214413 (2012).
- ⁸A. F. Kravets, Y. I. Dzhezherya, A. I. Tovstolytkin *et al.*, “Synthetic ferrimagnets with thermomagnetic switching,” *Phys. Rev. B* **90**, 104427 (2014).
- ⁹A. F. Kravets, D. M. Polishchuk, Y. I. Dzhezherya *et al.*, “Anisotropic magnetization relaxation in ferromagnetic multilayers with variable interlayer exchange coupling,” *Phys. Rev. B* **94**, 064429 (2016).
- ¹⁰A. F. Kravets, A. I. Tovstolytkin, Y. I. Dzhezherya *et al.*, “Spin dynamics in a Curie-switch,” *J. Phys. Condens. Matter* **27**, 446003 (2015).
- ¹¹A. A. Fraerman and I. A. Shereshevskii, “Magnetocaloric effect in ferromagnet/paramagnet multilayer structures,” *JETP Lett.* **101**, 618–621 (2015).
- ¹²S. N. Vdovichev, N. I. Polushkin, I. D. Rodionov, V. N. Prudnikov, J. Chang, and A. Fraerman, “High magnetocaloric efficiency of a NiFe/NiCu/CoFe/MnIr multilayer in a small magnetic,” *Phys. Rev. B* **98**, 014428 (2018).
- ¹³C. G. Robbins, H. Claus, and P. A. Beck, “Transition from ferromagnetism to paramagnetism in Ni-Cu alloys,” *J. Appl. Phys.* **40**, 2269–2273 (1969).
- ¹⁴K. E. Grew, “The specific heat of nickel and of some nickel-copper alloys,” *Proc. R. Soc. A* **145**, 509–522 (1934).
- ¹⁵M. Abramowitz and I. A. Stegun, *Handbook of Mathematical Functions*, Applied Mathematics Series Vol. 55 (National Bureau of Standards, Washington, 1964).
- ¹⁶N. Sorensen, R. E. Camley, and Z. Celinski, “Exchange stiffness as a function of composition in $\text{Cu}_x(\text{Ni}_{0.80}\text{Fe}_{0.20})_{1-x}$ alloys,” *J. Magn. Magn. Mater.* **477**, 344–349 (2019).
- ¹⁷G. B. Stenning, L. R. Shelford, S. A. Cavill, F. Hoffmann, M. Haertinger, T. Hesjedal, G. Woltersdorf, G. J. Bowden, S. A. Gregory, C. H. Back, P. A. J. de Groot, and G. van der Laan, “Magnetization dynamics in an exchange-coupled NiFe/CoFe bilayer studied by x-ray detected ferromagnetic resonance,” *New J. Phys.* **17**, 013019 (2015).
- ¹⁸A. F. Franco and P. Landeros, “Ferromagnetic resonance of an heterogeneous multilayer system with interlayer exchange coupling: An accessible model,” *J. Phys. D Appl. Phys.* **49**, 385003 (2016).
- ¹⁹X. Liu, W. Zhang, M. J. Carter, and G. Xiao, “Ferromagnetic resonance and damping properties of CoFeB thin films as free layers in MgO-based magnetic tunnel junctions,” *J. Appl. Phys.* **110**, 033910 (2011).
- ²⁰This equation is obtainable from the functional in Eq. (2) after eliminating the term responsible for non-uniform exchange and after adding the interaction with an applied magnetic field H (Zeeman energy).
- ²¹S. Michalski, R. Skomski, X.-Z. Li, D. Le Roy, T. Mukherjee, C. Binek, and D. J. Sellmyer, “Isothermal entropy changes in nanocomposite $\text{Co:Ni}_{67}\text{Cu}_{33}$,” *J. Appl. Phys.* **111**, 07A930 (2012).
- ²²N. I. Polushkin, I. Y. Pashenkin, E. Fadeev, E. Lahderanta, and A. A. Fraerman, “Magnetic and magnetocaloric properties of Py/Gd/CoFe/IrMn stacks,” *J. Magn. Magn. Mater.* **491**, 165601 (2019).